APPLIED PHYSICS LETTERS **91**, 202116 (2007)

Structural investigation of nitrided *c*-sapphire substrate by grazing incidence x-ray diffraction and transmission electron microscopy

Hyo-Jong Lee,[a)] Jun-Seok Ha,[a),b)] S. W. Lee, H. J. Lee, H. Goto, S. H. Lee, M. W. Cho,[a)] and T. Yao[a)]
Center of Interdisciplinary Research, Tohoku University, 6-3 Aoba, Aramaki, Aoba-ku, Sendai 980-8578, Japan

T. Minegishi and T. Hanada
Institute for Materials Research, Tohoku University, 2-1-1 Katahira, Aoba-ku, Sendai 980-8577, Japan

Soon-Ku Hong
School of Nanoscience and Technology, Chungnam National University, Daejeon 305-764, Korea

Osami Sakata
Japan Synchrotron Radiation Research Institute (JASRI), 1-1-1 Kouto, Sayo-cho, Sayo-gun, Hyogo 679-5198, Japan

Jae Wook Lee and Jeong Yong Lee
Department of Materials Science and Engineering, Korea Advanced Institute of Science and Technology, Daejeon 305-701, Korea

(Received 16 August 2007; accepted 31 October 2007; published online 16 November 2007)

A grazing incidence x-ray diffraction with a synchrotron radiation and a cross-sectional high-resolution transmission electron microscopy were performed on the sapphire surface nitrided at 1080 °C for 30 min. The thickness of the nitrided layer was about 2 nm. It was found out that the wurtzite, zinc-blende, and 30° rotated zinc-blende aluminum nitrides were formed on the sapphire surface. The 30° rotated zb-AlN formed the incoherent interface and has higher activation energy of formation, while the nonrotated zb-AlN formed the coherent interface. © *2007 American Institute of Physics*. [DOI: 10.1063/1.2815919]

The nitridation treatment and the low temperature deposition of GaN were sequentially performed on the sapphire substrate before the main growth of high temperature GaN.[1] Keller and co-workers reported that the metalorganic chemical vapor deposition grown GaN on the longer nitridation of sapphire at 1050 °C showed two orders of higher dislocation density, yellow band luminescence, low Hall mobility, and high carrier concentration than the GaN film with the shorter nitridation.[2,3] In order to understand the nitridation effect, first of all, it is highly needed to find out the overall chemical compounds formed on the nitrided sapphire surface and each crystalline orientation relationship. Although x-ray diffraction (XRD) method is generally used to find them, it is very hard to detect any peak by conventional XRD because the thickness of the nitrided layer is normally below several nanometers. Therefore, investigations based on surface sensitive or nanoscale accessible instruments such as x-ray photoelectron spectroscopy, reflection high-energy electron diffraction, and transmission electron microscopy (TEM) have been performed.[4,5] In this letter, in order to investigate crystallographic and structural properties of the nitrided sapphire substrates in detail, a grazing incidence x-ray diffraction (GIXD) measurement was performed. It was found out that the wurtzite aluminum nitride (*w*-AlN) and the nonrotated and 30° rotated zinc-blende AlN (zb-AlN) against the sapphire substrate were formed by nitridation. The nitrided sapphire sample was also investigated by high-resolution TEM (HRTEM) to confirm the results obtained by XRD.

The nitridation of sapphire substrate was performed at 1080 °C by supplying an ammonia gas with a flow rate of 0.5 l/min for 30 min. Figure 1 is glancing incident x-ray diffraction results for $\Phi/2\theta\chi$ axes with alignment for sapphire $(11\bar{2}0)$ and $(30\bar{3}0)$ for the nitrided sapphire $\lambda = 0.9987$ Å. Here, we can see that both *w*-AlN $(10\bar{1}0)$ and zb-AlN (422) planes are parallel to the sapphire $(11\bar{2}0)$ plane, and also, both *w*-AlN $(11\bar{2}0)$ and zb-AlN (220) planes are parallel to the sapphire $(30\bar{3}0)$ plane. That is, orientation relationships between the *w*-AlN, sapphire, and zb-AlN are determined to be $(10\bar{1}0)_{w\text{-AlN}} \| (11\bar{2}0)_{\text{sapphire}} \| (211)_{\text{zb-AlN}}$ and $(11\bar{2}0)_{w\text{-AlN}} \| (10\bar{1}0)_{\text{sapphire}} \| (110)_{\text{zb-AlN}}$. The observed relationship between the *w*-AlN formed by nitridation and the sapphire substrate is well agreed with the prior reports for the 300 nm thick *w*-AlN deposited on the sapphire substrate.[6,7] Here, it should be mentioned that it was convinced that from the appearances of *w*-AlN $(10\bar{1}0)$ and $(20\bar{2}0)$ peaks, the *w*-AlN was formed on the sapphire surface, whereas it was not possible to know whatever the zb-AlN was formed or not because the zb-AlN (422), (220), and (440) planes have very similar interplanar spacings with the *w*-AlN $(30\bar{3}0)$, $(11\bar{2}0)$, and $(22\bar{4}0)$ planes, respectively. Here, it should be noted that there was an additional peak between the two peaks of the sapphire $(11\bar{2}0)$ and the *w*-AlN $(20\bar{2}0)$, as marked by a red arrow in Fig. 1(a). The position of the additional peak was well matched to a *w*-AlN $(11\bar{2}0)$ or a zb-AlN $(2\bar{2}0)$ plane. If the additional peak was regarded as a *w*-AlN $(11\bar{2}0)$ plane, the *w*-AlN $(10\bar{1}0)$ peak should be appeared in Fig. 1(b) ac-

[a)]Also at Institute for Materials Research, Tohoku University, 2-1-1 Katahira, Aoba-ku, Sendai, 980-8577, Japan.
[b)]Electronic mail: jsha@cir.tohoku.ac.jp

 © 2007 American Institute of Physics
Downloaded 14 Apr 2011 to 143.248.103.56. Redistribution subject to AIP license or copyright; see http://apl.aip.org/about/rights_and_permissions

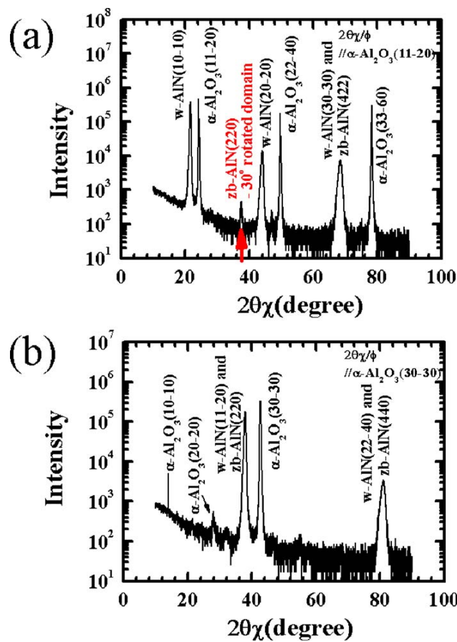

FIG. 1. (Color online) Glancing incident x-ray diffraction results for the nitrided sapphire. (a) Alignment for sapphire {11-20} and (b) for sapphire {30-30}.

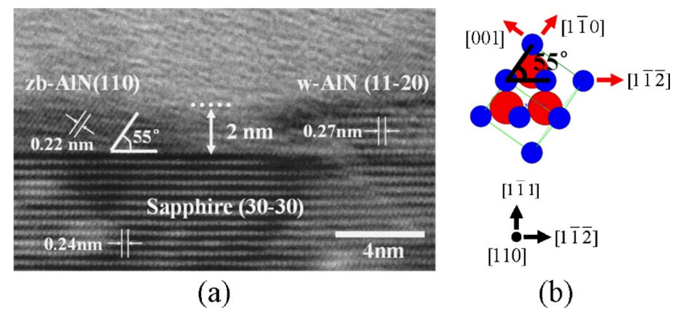

FIG. 2. (Color online) Cross-sectional HRTEM image on the nitrided sapphire. (a) A HRTEM image, and (b) a schematic diagram for the zinc-blende AlN projected on {110} plane.

quired with $\Phi/2\theta\chi\|$ sapphire ($30\bar{3}0$). However, *w*-AlN ($10\bar{1}0$) peak was not observed in Fig. 1(b). Otherwise, if the additional peak stood for zb-AlN ($2\bar{2}0$), the zb-AlN ($2\bar{4}2$) peak should be in Fig. 1(b) because zb-AlN ($1\bar{2}1$) peak was forbidden. However, the zb-AlN ($2\bar{4}2$) peak was also not observed in Fig. 1(b). The peak of zb-AlN ($2\bar{4}2$) seemed not to be detected from the random intensity because the peak intensity of zb-AlN ($2\bar{4}2$) would be considerably low by reason of relatively high indices. Therefore, we concluded that the additional peak should be the zb-AlN ($2\bar{2}0$) plane. Additionally, in order that the zb-AlN ($2\bar{2}0$) was matched to the sapphire ($11\bar{2}0$), the zb-AlN (111) plane was rotated by 30° for the sapphire (0006) plane with respect to the atomic configuration of the close-packed plane.

In order to confirm the formation of zb-AlN, HRTEM measurement was performed on the sample, as shown in Fig. 2. Figure 2 showed a HRTEM micrograph for the nitrided sapphire. First, we could see about 2 nm thick nitrided layer on the sapphire substrate formed by nitridation. Second, it was found out that the *w*-AlN and the zb-AlN were formed equivalently on the sapphire surface. The hexagonal and cubic structures were easily discernible by their typical lattice fringes. The observed interplanar *d* spacings of approximately 0.22 and 0.27 nm corresponded well to those of the (001) plane of zb-AlN and the ($1\bar{1}00$) plane of *w*-AlN, respectively. Figure 2(b) showed the schematic diagram of the zb-AlN atomic structure projected on the [110] direction, and the red and blue spheres represented the aluminum and nitrogen atoms, respectively. The (100) lattice fringes of zb-AlN were inclined by about 55° which agreed well with the tilt angle of 54.74° between [$1\bar{1}0$] and [$1\bar{1}\bar{2}$], as shown in Fig. 2(b). From Fig. 2, we could know that the cross-sectional direction of sapphire [$30\bar{3}0$] was parallel to those of *w*-AlN [$11\bar{2}0$] and zb-AlN [110], and the right hand direction of sapphire [$11\bar{2}0$] was parallel to those of *w*-AlN [$1\bar{1}00$] and zb-AlN [$1\bar{1}\bar{2}$].

The *d* spacing calculated from the peak position in Fig. 1 and its difference ratios were summarized in Table I. The difference ratio was defined by $(D_{meas}-D_{ref})/D_{ref}$. Here, D_{meas} and D_{ref} mean the measured and reference *d* spacings, respectively. Therefore, the difference ratio has a similar meaning of the elastic strain along the normal direction of the plane which the peak position stood for.[8,9] All the difference ratios of the *w*-AlN and zb-AlN except the 30° rotated zb-AlN were negative, which meant that the compressive strain was developed in the *w*-AlN and the zb-AlN. The compressive strain was mostly attributed to the difference between the atomic distances of sapphire and *w*-AlN (or zb-AlN). The average length of O–O bondings on {0006} plane of the sapphire is 2.747 Å,[10] and the length of N–N bonding on {0002} plane of the *w*-AlN is 3.112 Å (3.087 Å for the zb-AlN {111} plane).[8,9] The bonding length of sapphire is smaller by about 12% and 11% than those of *w*-AlN and

TABLE I. Calculation of *d* spacing and the difference ratio. The difference ratio means that the difference between the measured and reference *d* spacings for each AlN plane is divided by the reference *d* spacing.[a,b]

Al_2O_3 index	AlN index	*D* (meas) (Å)	*D* (ref) (Å)	Ratio of difference (%)
(11–20)	*w*-AlN (10-10)	2.662	2.695	−1.21
	zb-AlN (220)	1.552	1.543	0.56
	w-AlN (20-20)	1.330	1.348	−1.33
	w-AlN (30-30) and zb-AlN (224)	0.887	0.898 and 0.891	−1.31 and −0.50
(30–30)	*w*-AlN (11-20) and zb-AlN (220)	1.539	1.556 and 1.543	−1.07 and −0.26
	w-AlN (22-40) and zb-AlN (440)	0.767	0.778 and 0.772	−1.35 and −0.54

[a]Reference 7.
[b]Reference 8.

Downloaded 14 Apr 2011 to 143.248.103.56. Redistribution subject to AIP license or copyright; see http://apl.aip.org/about/rights_and_permissions

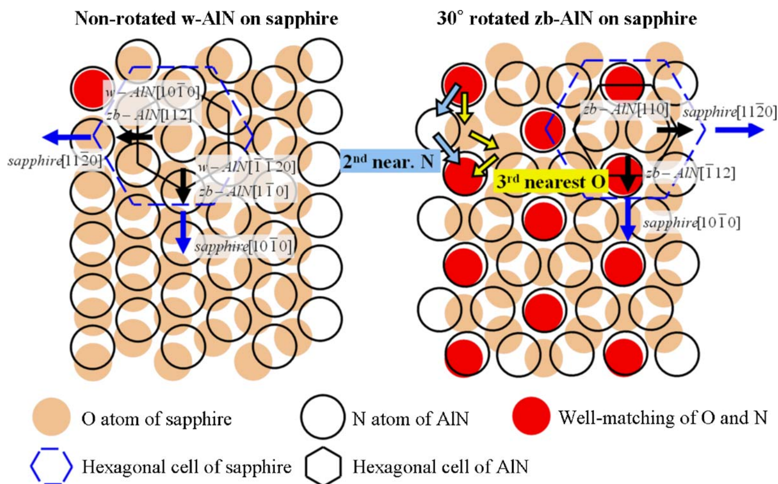

FIG. 3. (Color online) Schematic diagram of N atomic layer of the nonrotated *w*-AlN {0002} and 30° rotated zb-AlN {111} planes overlapped on the O atomic layer of sapphire {0006} plane.

zb-AlN, respectively. Therefore, the initial misfit strains of *w*-AlN and zb-AlN should be compressive. The other factor is the thermal expansion difference ($\Delta\alpha$) between AlN and sapphire. Because the thermal expansion difference of zb-AlN could not be found for the reference, considering only that of *w*-AlN, the $\Delta\alpha$ between *w*-AlN and sapphire is 3.1×10^{-6} K^{-1}. The estimated thermal strain of *w*-AlN for sapphire is about 0.33% in our experimental conditions. Therefore, considering the comparison to the difference ratio in Table I and assuming similar physical properties of the *w*-AlN and the zb-AlN, the main origin of the compressive strain in the *w*-AlN and zb-AlN might result from the difference of the interatomic bonding length.[11,12]

Here, it should be noted that the *d*-spacing difference of the 30° rotated zb-AlN was positive. In order to understand a meaning of the observed positive value, we considered the atomic configuration on the 30° rotated zb-AlN with the sapphire substrate. Figure 3 shows schematic atomic configurations of AlN on sapphire. Because the *w*-AlN {0002} and the zb-AlN {111} have a similar atomic configuration with the close-packed plane, for convenience of expression, the case of the *w*-AlN was considered. Here, the N atom layers of the nonrotated *w*-AlN {0002} and 30° rotated zb-AlN {111} planes were overlapped on the O atom layer of sapphire {0006} plane, assuming that the Al atom layers at the interlayer between two layers of O and N atoms were excluded. In the case of the nonrotated *w*-AlN (or zb-AlN) and the sapphire, it was found out that the configurational mismatch of atoms gradually increased from a matching position of N and O atoms, and the initial misfit strain was developed. Conversely, in case of the 30° rotated zb-AlN and the sapphire, each atomic configuration was periodically well matched. It was also found out that the initial misfit strain of the 30° rotated zb-AlN was a little tensile because the O–O interatomic distance (5.495 Å) between an O atom and its third nearest atom was larger by only 2% than the N–N interatomic distance (5.390 Å) between a N atom and its second nearest atom. These results were in good agreement with the tendency of *d*-spacing difference ratios in Table I. In addition, from Fig. 1, it was known that the intensity of the *w*-AlN (20$\bar{2}$0) peak was larger by 30 times than that of its adjacent zb-AlN (2$\bar{2}$0) peak. Therefore, it seemed that it was difficult to find out the existence of the 30° rotated zb-AlN in the HRTEM observation.

Figure 3 shows that the nonrotated zb-AlN is fully coherent with the sapphire, as shown in Fig. 3(a), and with respect to the dangling bonding, it was thought that the interfacial energy of the nonrotated zb-AlN was much lower than that of the 30° rotated zb-AlN with the incoherent interface. It meant that the energy barrier of the nonrotated zb-AlN was much smaller than that of the 30° rotated zb-AlN. Therefore, it could be surmised that the nonrotated zb-AlN appeared dominantly because of such a lower-energy barrier.[13]

In summary, through the GIXD investigation of the synchrotron radiation and TEM measurement, it was found out that the *w*-AlN, nonrotated zb-AlN, and 30° rotated zb-AlN were formed on the nitrided sapphire surface. Considering the atomic configurations, the 30° rotated zb-AlN shall form the incoherent interface while the nonrotated zb-AlN shall form the coherent interface.

The synchrotron radiation experiments were performed at the BL13XU in the SPring-8 with the approval of the Japan Synchrotron Radiation Research Institute (JASRI) (Proposal No. 2007A1819).

[1]L. Liu and J. H. Edgar, Mater. Sci. Eng., R. **37**, 61 (2002).
[2]S. Keller, B. P. Keller, Y.-F. Wu, B. Heying, D. Kapolnek, J. S. Speck, U. K. Mishra, and S. P. DenBaars, Appl. Phys. Lett. **68**, 1525 (1996).
[3]B. Heying, X. H. Wu, S. Keller, Y. Li, D. Kapolnek, B. P. Keller, S. P. DenBaars, and J. S. Speck, Appl. Phys. Lett. **68**, 643 (1996).
[4]K. Uchida, A. Watanabe, F. Yano, M. Kouguchi, T. Tanaka, and S. Minagawa, J. Appl. Phys. **79**, 3487 (1996).
[5]P. Vennéguès and B. Beaumont, Appl. Phys. Lett. **75**, 4115 (1999).
[6]K. Dovidenko, S. Oktyabrsky, J. Narayan, and M. Razeghi, J. Appl. Phys. **79**, 2439 (1996).
[7]C. J. Sun, P. Kung, A. Saxler, H. Ohsato, K. Haritos, and M. Razeghi, J. Appl. Phys. **75**, 3964 (1994).
[8]W. Paszkowicz, S. Podsiadło, and R. Minikayev, J. Alloys Compd. **382**, 100 (2004).
[9]C.-Y. Yeh, Z. W. Lu, S. Froyen, and A. Zunger, Phys. Rev. B **46**, 10086 (1992).
[10]P. Thompson, D. E. Cox, and J. B. Hastings, J. Appl. Crystallogr. **20**, 79 (1987).
[11]H. Harima, J. Phys.: Condens. Matter **14**, R967 (2002).
[12]W. M. Yim, and R. J. Paff, J. Appl. Phys. **45**, 1456 (1974).
[13]D. A. Porter and K. E. Easterling, *Phase Transformations in Metals and Alloys*, 2nd ed. (Chapman and Hall, London, 1992), pp. 263–308.

Downloaded 14 Apr 2011 to 143.248.103.56. Redistribution subject to AIP license or copyright; see http://apl.aip.org/about/rights_and_permissions